TECHNICAL MEMORANDUM 376

MAY 1966

A CONDUCTING-SLAB MODEL FOR ELECTROMAGNETIC PROPAGATION WITHIN A JUNGLE MEDIUM

D.L. Sachs
P.J. Wyatt

DEFENSE RESEARCH CORPORATION
6300 Hollister Avenue
P.O. BOX 3587 • SANTA BARBARA, CALIFORNIA • 93105

GENERAL RESEARCH CORPORATION
P.O. Box 3587
Santa Barbara, California 93105

PREFACE

As one element of a continuing program to study AGILE communication requirements, Defense Research Corporation has been analyzing the transmission of radio signals through heavily vegetated (jungle) terrains. The major objective of this work is to devise theoretical models that can be used to predict the signal strengths to be expected in a variety of practical situations. Our program to accomplish this examines the electromagnetic characteristics of particular models of the propagation medium and then tests the usefulness of the model by its ability to represent experimentally available results in a meaningful way.

Beginning with the simplest possible model, we are introducing increasing levels of sophistication as required by the comparison with experiment. For example, in the initial phase, the transmission medium was represented as an infinite, homogeneous region, (see Ref. 2 of the present report), characterized only by a complex dielectric constant. In this report, a somewhat more complicated model is analyzed: a uniform slab, of thickness corresponding to the height of the jungle, bounded on one side by an infinite lossless region (air), and on the other side by an infinite, lossy region (ground). Further refinements will be introduced in the future.

This program is under the direction of Dr. B. A. Lippmann. The work reported on here was carried out by Drs. D. L. Sachs and P. J. Wyatt, with substantial assistance from Dr. P. J. Redmond.

ABSTRACT

A theoretical determination of the path loss in radio propagation through jungle is obtained by considering the jungle as a homogeneous conducting dielectric slab on a flat earth. An exact integral is obtained for the vertical component of the electric field within the jungle due to a vertical electric dipole within the jungle. An analytic evaluation of the integral leads to an approximate expression for the field and an estimate of the error. When this accuracy is insufficient, a numerical evaluation of the integral is performed. The combination of analytic and numerical techniques leads to the evaluation of the electric field and thereby path loss to any accuracy desired. Experimental measurements of path loss in a Thailand jungle are compared with the calculations. The results agree within a standard deviation of 6 db when the jungle conductivity is taken as 0.15 millimho/m.

CONTENTS

I. INTRODUCTION

The practical difficulties associated with radio communications in regions of dense vegetation have been recognized for some time.[1] The vegetation has a high water content so that the jungle medium is lossy. If the radio waves propagated along a direct path through the medium the received signal would be exponentially attenuated.[2] With reasonable values of the conductivity ($\sigma \simeq 100$ μmho/m) the attenuation is approximately 0.2 db/m at one megacycle and is even greater at higher frequencies. Such a high attenuation would effectively prevent radio communication over distances greater than a few thousand feet. Since radio communication does exist over greater distances than this, albeit quite poorly on occasion, there has been speculation that the radiation propagates for the most part in the air above the jungle.

This paper derives from first principles expressions for the propagation between two antennas immersed in a jungle-like medium. The theory is compared with experiments conducted in a Thai jungle by Jansky and Bailey[3,4] and the apparent anomaly referred to appears to be explained.

The electrical properties of a jungle are extremely complicated. Most of the space is occupied by air with properties close to the vacuum. The trees and other vegetation have a higher conductivity and dielectric constant and are distributed more or less randomly over the surface. Fortunately, at long wavelengths the propagation characteristics of an electromagnetic wave are not sensitive to this fine detail. An electromagnetic wave propagating through a medium is only sensitive to some average properties of the medium where the average is taken over regions whose linear dimensions are of the order of a wavelength.[2]

We therefore, consider an approximation to the jungle consisting of a uniform slab of fixed height with permitivity ε_j and conductivity σ_j bounded by a flat earth surface with permitivity ε_g and conductivity σ_g and above by the air with vacuum properties. This picture is reasonable provided:

1. The fluctuation in the number of trees, etc., in an area one wavelength squared is small compared to the total number of trees in this area.

2. If the height of the jungle is larger than a wavelength it is necessary that, within the jungle, the average electrical properties do not vary significantly with height.

3. The transition region between the air above and the jungle must be small compared to a wavelength.

These conditions are probably sufficient to guarantee the qualitative validity of the theory. For quantitative validity it would also be necessary that the terrain be reasonably level over the range and that the properties of the jungle be reasonably uniform over the range.

In this study it was intended to determine the range of validity of this idealized slab model by comparing the results of calculations with experimental data. For the wavelength region studied so far (wavelength from 3 to 50 meters) we have obtained satisfactory agreement between theory and experiment.

The problem of the propagation of electromagnetic energy through a many-layered medium has been studied extensively.[5,6,7] For this general class of problems it is relatively easy to obtain a formal solution to the problem in which the field strength at the receiver is represented by an integral. We have obtained such an integral representation for the particular geometry of our problem.

Unfortunately, the integral representation of the solution is sufficiently complicated that considerable effort is required before numerical results can be obtained in a form suitable for comparison with experiment. We have performed these calculations with sufficient precision so that any discrepancy between the mathematical results and the

experimental data is due either to inadequacies in the physical model or uncertainties in the experiment.

At larger ranges it is possible to obtain an approximate analytical evaluation of the integral and an estimate of the error involved in the approximation. This asymptotic solution corresponds to a lateral wave propagation mode, or "treetop" mode. This mode may be described in terms of a wave packet (ray) which propagates up to the treetops, striking the boundary near the critical angle for total internal reflection. It then propagates in the air until it reenters at an angle near the critical angle. The field is attenuated exponentially only along a path from the transmitter to the treetops and from the treetops to the receiver. While propagating through the air the field falls off as $1/r^2$.

This asymptotic formula is capable of explaining most of the experimental data. At the smaller ranges the error becomes too large. For this region the original integral was evaluated by numerical quadrature. As a check on the consistency of the two procedures the numerical quadrature was carried up to ranges where the asymptotic formula was valid. In the region of overlap the two methods gave identical results. Examples where all of these numerical techniques are required are given in Sec. III, and the transition regions are discussed.

In Sec. II the formal mathematical solution is presented and it is demonstrated that this solution is consistent with our description of the lateral waves.

In Sec. III the path loss for a variety of experimental data is compared with the theoretical predictions. To date we have considered only the cases where both the receiving and transmitting antennas were in the jungle medium. There is a considerable amount of data for this case and it is in this situation where the greatest difficulties in communication might be anticipated. The calculations considered only

the case of vertical polarization, a frequency range from 6 to 100 Mc/sec, and a range up to one mile. Within these restrictions the available data provided by Jansky and Bailey was considered. The theoretical results depend most critically on the jungle conductivity and this was the only parameter varied. The theoretical and experimental results agree to within a standard deviation of 6 db when the jungle conductivity is taken as 0.15 millimho/m. This agreement is considered satisfactory. Jansky and Bailey performed independent measurements corresponding to the same range, height of antennas, and frequency with results varying by as much as 13 db.

The average conductivity of the Thailand jungle has not been measured, and there are very few measurements of this kind available for any jungle. The value we have obtained is reasonable and is consistent with experimental results[8] obtained in California.

The slab model predictions appear to provide a satisfactory correlation with the experimental data. Indeed the model works well for wavelengths shorter than we had at first anticipated and we intend to extend our calculations to still shorter wavelengths in order to determine when and if the model seriously breaks down. We also intend to consider horizontal polarizations and cases where one or both of the antennas are above the jungle.

The details of the numerical evaluations and the derivation of the formal solution are contained in appendices.

II. PHYSICS OF THE SLAB MODEL

The mathematical problem posed by the idealized physical situation possesses an exact formal solution. It suffices to consider only the formula for the z-component of the electric field, since the other field components are readily obtained from E_z. The z component of the electric field at the receiver is given by

$$E_z = P \int_{-\infty}^{+\infty} \alpha^3 H_o^{(1)}(\alpha R) F(\alpha) \, d\alpha \quad \text{volt/m} \tag{1}$$

where $P = \frac{\pi i f}{n^2}$ (power radiated in kw)$^{1/2}$ and f is the frequency in Mc.

For both the receiving and transmitting antenna in the jungle

$$F(\alpha) = \frac{1}{x_j}\left[e^{-x_j X} + \left(V_g e^{-x_j Y} + V_a e^{-x_j(2H-Y)} + V_a V_g e^{-x_j(2H+X)} + V_a V_g e^{-x_j(2H-X)}\right) \Big/ \left(1 - V_a V_g e^{-x_j 2H}\right)\right] \tag{2}$$

where

$$V_a = \frac{x_j - n_j^2 x_a}{x_j + n_j^2 x_a} \qquad V_g = \frac{n_g^2 x_j - n_j^2 x_g}{n_g^2 x_j + n_j^2 x_g}$$

where $n^2 = \varepsilon + 18\, i\sigma$ (millimho/m)/f(Mc). (See Fig. 1.) This integral represents the solution in the jungle as a superposition of cylindrical waves which are successively reflected from the jungle-air and jungle-ground interfaces with reflection coefficients V_a and V_g respectively. The variable of integration, α, is the cylindrical propagation constant.

Distances are measured in units $c/\omega = 150/(\pi f) = 1/K_o$

and $R = K_o r$, $H = K_o h$, $X = K_o|z-z_o|$, $Y = K_o(z+z_o)$, $Z = K_o z$, $Z_o = K_o z_o$.

The attenuation factors for different paths are described in terms of the variables

$$x_j = \sqrt{\alpha^2 - n_j^2}, \quad x_a = \sqrt{\alpha^2 - 1} \quad \text{and} \quad x_g = \sqrt{\alpha^2 - n_g^2}$$

and the square roots are defined so that the real parts of the x's are positive.

THE STRATIFIED MODEL OF THE JUNGLE COMMUNICATION MEDIUM

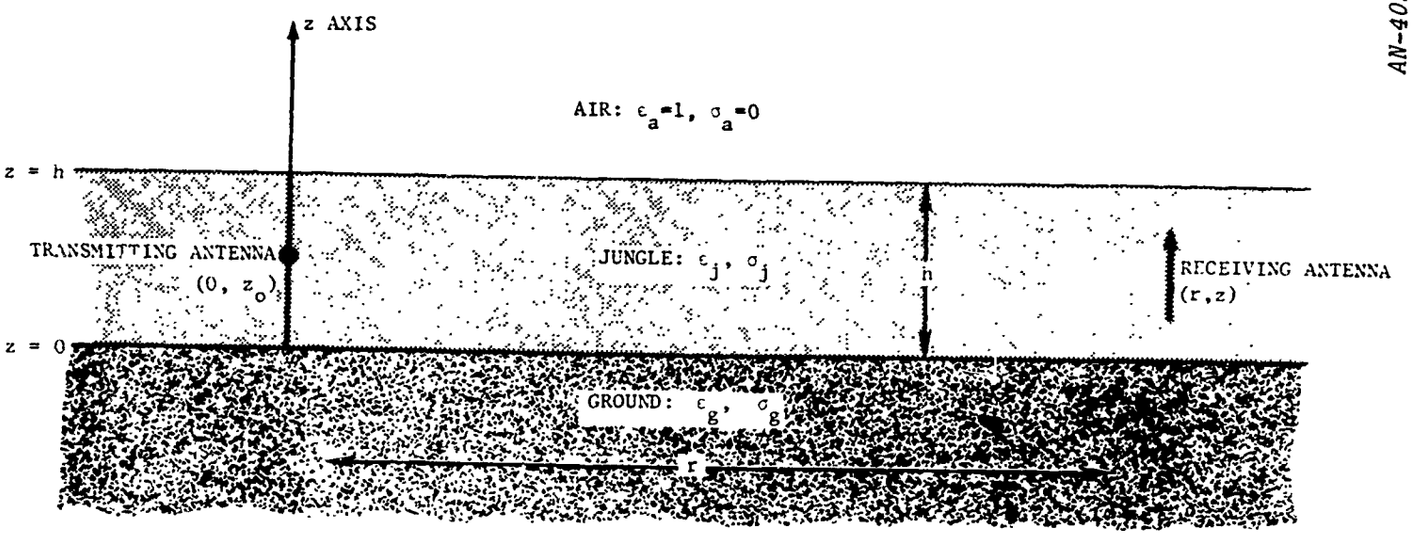

UNCLASSIFIED

Figure 11. The Stratified Model of the Jungle Communications Medium.

The various terms in Eq. (2) have a simple interpretation. The first term $e^{-x_j X}$ represents the field produced by the dipole in the absence of the interfaces. The next term proportional to $V_g e^{-x_j Y}$ represents those plane waves which are reflected an odd number of times with the first reflection occurring at the ground. The remaining terms represent cases where there is an odd number of reflections with the first reflection at the air interface, an even number of reflections with the first reflection at the air interface, and an even number of reflections with the first reflection at the ground interface. The numerators represent the results of the first one or two reflections respectively and the denominator sums the contributions from all subsequent pairs of reflections from the ground and air interfaces.

For most values of the parameters the integrand in Eq. (1) is strongly peaked at $\alpha = 1$ corresponding to a ray, called the lateral wave, propagating at the angle of total internal reflection. In such cases the integral may be approximated by a simpler integral describing this ray. The new integral can be evaluated easily by a Gaussian quadrature. An approximate analytical evaluation of the new integral can also be performed. Such solutions are presented in Appendix III and the domains of their validity are discussed.

When the methods described above break down, it becomes necessary to evaluate the original integral, Eq. (1), numerically. This is a difficult task because the integrand is oscillatory. Methods for accurately evaluating such oscillatory integrals are available and they were applied to this type of problem for the first time in this study.

When the solution can be expressed in terms of the superposition of a set of plane waves with propagation vectors lying in a small region of k-space it is most appropriate to interpret the solution in terms of a wave packet which suffers successive reflections. In order to gain

some insight into the nature of these solutions we consider the behavior of a wave packet after a single reflection.

Consider a wave packet with average propagation vector $\vec{k}^o$ incident on a plane boundary as in Fig. 2. For simplicity we assume the fields are independent of y. The incident wave packet can then be described by

$$E_z^{inc}(x,z,t) = \int dk_x dk_z \, A(k_x,k_z) \, \text{expi}(k_x x + k_z z - \omega t) \tag{3}$$

where ω is a function of k_x and k_z and the function A is strongly peaked at $\vec{k} = \vec{k}^o$. If we expand the phase factor about the point $\vec{k} = \vec{k}^o$, we obtain

$$E_z^{inc}(x,z,t) = e^{ik_x^o x + ik_z^o z - i\omega^o t} \, f\left(x - \frac{\partial\omega}{\partial k_x} t, \; z - \frac{\partial\omega}{\partial k_z} t\right) \tag{4}$$

where $\partial\omega/\partial k_x$ and $\partial\omega/\partial k_z$ are components of the group velocity evaluated at $\vec{k}^o$ and

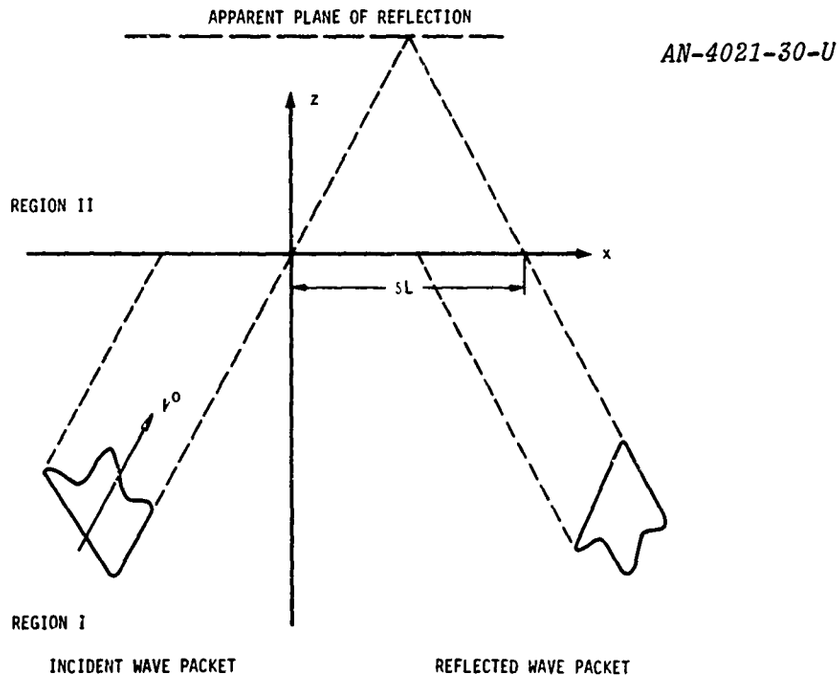

Figure 2. Displacement of Wave Packet

$$f(\alpha,\beta) = \int dk_x dk_z \; A(k_x,k_z) \exp i \left[(k_x-k_x^o)\alpha + (k_z-k_z^o)\beta\right] \qquad (5)$$

The reflected wave is given by

$$E^{ref}(x,z,t) = \int dk_x dk_z \; A(k_x,k_z)|V(k_x,k_z)|\exp i\,(k_x x - k_z z - \omega t + \phi(k_x,k_z)) \qquad (6)$$

where the reflection coefficient is $|V|e^{i\phi}$. If we assume that the amplitude of the reflection coefficient varies sufficiently slowly so that it may be taken outside the integral we obtain

$$E^{ref}(x,z,t) = |V(k_x^o,k_z^o)|\; e^{i(k_x^o x - k_z^o z - \omega^o t + \phi(k_x^o,k_z^o))}$$

$$\cdot\; f\left(x - \frac{\partial\omega}{\partial k_x} t + \frac{\partial\phi}{\partial k_x}\,,\; -z - \frac{\partial\omega}{\partial k_z} t + \frac{\partial\phi}{\partial k_z}\right) \qquad (7)$$

where f is the same function that occurs in Eq. (4) and the derivatives are again evaluated at $\vec{k}^o$.

Consider now an incident wave packet which first strikes the boundary at t = 0 and at this time is nonvanishing only for negative x and z. These conditions require

$$f(\alpha,\beta) = 0 \quad \text{if} \quad \alpha > 0 \quad \text{or} \quad \beta > 0.$$

By examining Eq. (7) we see that the reflected signal will not appear in region I (illustrated in Fig. 2), until a sufficient time has elapsed so that the second argument of f is negative at z = 0. This time delay is given by

$$\delta T = (\partial\phi/\partial k_z) \;/\; (\partial\omega/\partial k_z).$$

When the field reappears, the wave packet has traveled a lateral distance δL obtained by setting the first argument of f equal to zero. The transverse displacement is given by

$$\delta L = -\partial\phi/\partial k_x + (\partial\omega/\partial k_x)\ \delta T.$$

This lateral mode, or "treetop mode," dominates at large distances because it propagates mainly in the lossless medium rather than in the jungle. The effect will be a large one only when the phase ϕ is a rapidly varying function of either the frequency or angle. In our problem this occurs at the critical angle θ_c of total internal reflection. At $\theta = \theta_c$, $\delta L = \infty$ and is a rapidly varying function of the difference $\theta - \theta_c$.

By looking in detail at the dependence of δL on θ it is possible to demonstrate that the field strength varies as $\delta r^{-1/2}\ \delta L^{-3/2}$ which is consistent with the analytically obtained dependence of $1/r^2$.

The above analysis is by no means novel or original. The phenomenon is a general characteristic of wave motion and whenever the phase of a wave is a function of any parameter there will be a displacement in the corresponding "canonically conjugate" parameter. In electrical network theory the time delay associated with a phase change which varies rapidly with frequency is very familiar. In quantum mechanics the rapid energy variation of a phase shift at a resonance is associated with the time the particle spends in the resonant state. The lateral displacement of a light beam has been observed for rays near the critical angle, and this kind of a wave is well known in seismology.

In our discussion it was necessary to make the assumption that the magnitude of the reflection coefficient varied slowly with angle. Such an assumption is correct for a lossless medium but is not valid if there are significant losses. Such losses would change the shape of

the wave packet. Other effects, such as a spherical divergence of the wave packet, which change the shape of the wave packet have also been ignored. The formal solution correctly contains all these effects. As a result these considerations are an aid in the understanding of the analytical calculations but do not in any sense replace them.

The formal solution is originally expressed as an integral over real α. In this form the numerical quadrature described in Appendix II is appropriate. The integral may also be considered as a contour integral in the complex plane. By deforming the contour, contributions from discrete poles and branch cuts may be identified and separately considered. This is discussed in detail in Appendix III. The pole terms correspond to damped waveguide modes. For sufficiently large r the contributions from the branch cuts correspond to the lateral waves as described above. At smaller r the contribution from the branch cuts has a more complicated behavior than described above and represents an extension of these simple ideas.

III. SAMPLE CALCULATIONS AND PRELIMINARY COMPARISON WITH EXPERIMENT

Figure 3 is a plot of calculated E_z(rms) vs range for a frequency of 0.88 Mc. For this low frequency, the numerical integration described in Appendix II must be used throughout the range of interest. Figure 3 illustrates three distinct stages of the behavior of E_z vs r. For $r < 10^2$m, E_z decreases exponentially. In this region the waves remain in the jungle and are described mathematically by the pole terms. For $10^2\text{m} < r < 10^3\text{m}$, E_z decreases as 1/r. The pole terms are now negligible compared to the lateral wave which has a 1/r dependence at short ranges. For $10^3\text{m} < r < 10^4\text{m}$, the r dependence of the lateral wave is in a transition region which will lead to the final dependence of $1/r^2$ given by Eq. (40), Appendix III for $r > 10^4$m.

Figure 4 illustrates this transition for f = 2 Mc. The points marked with an x are the result of the Gaussian integration of the

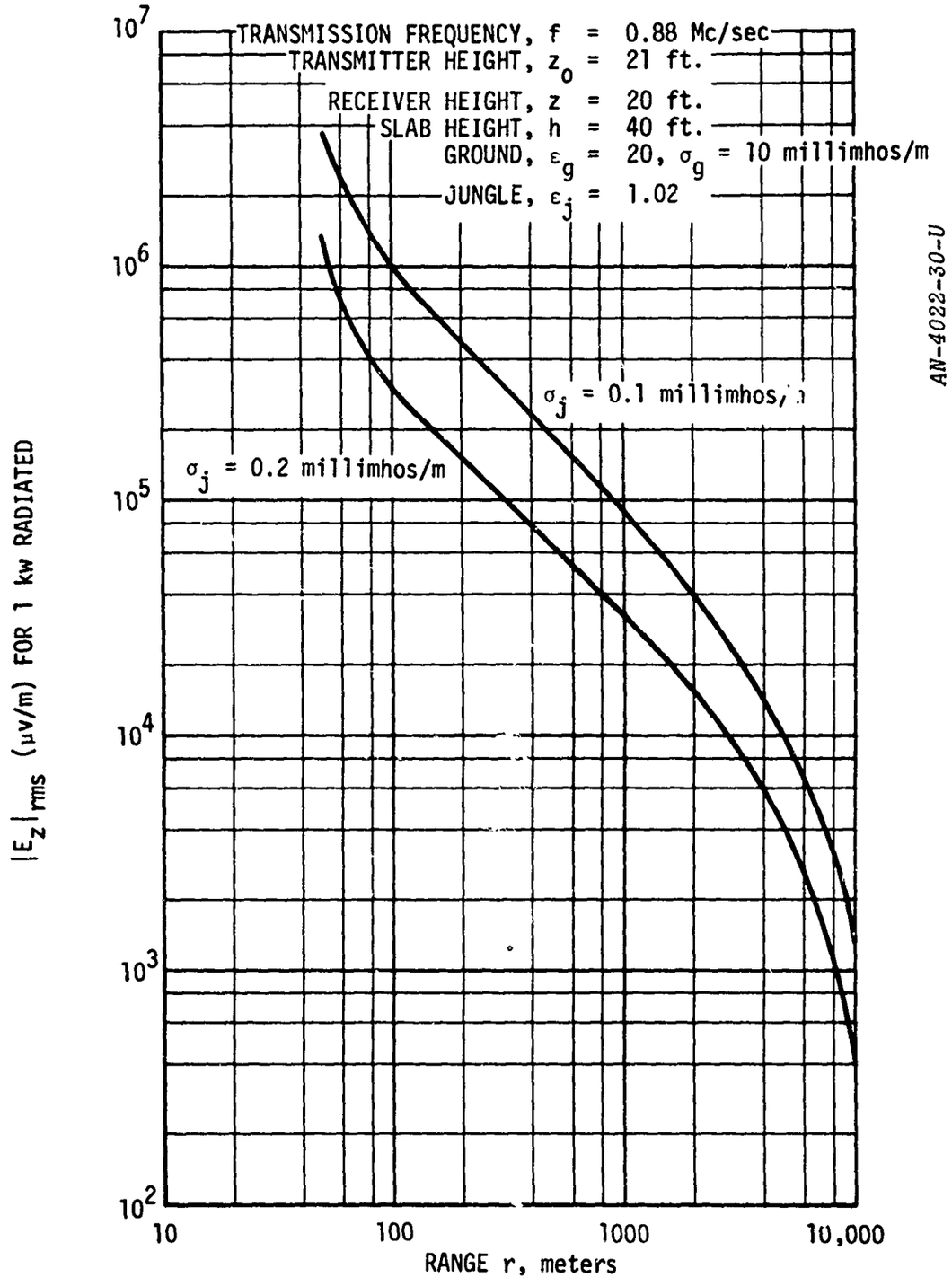

Figure 3. Sample Calculated Field for f = 0.88 Mc/sec

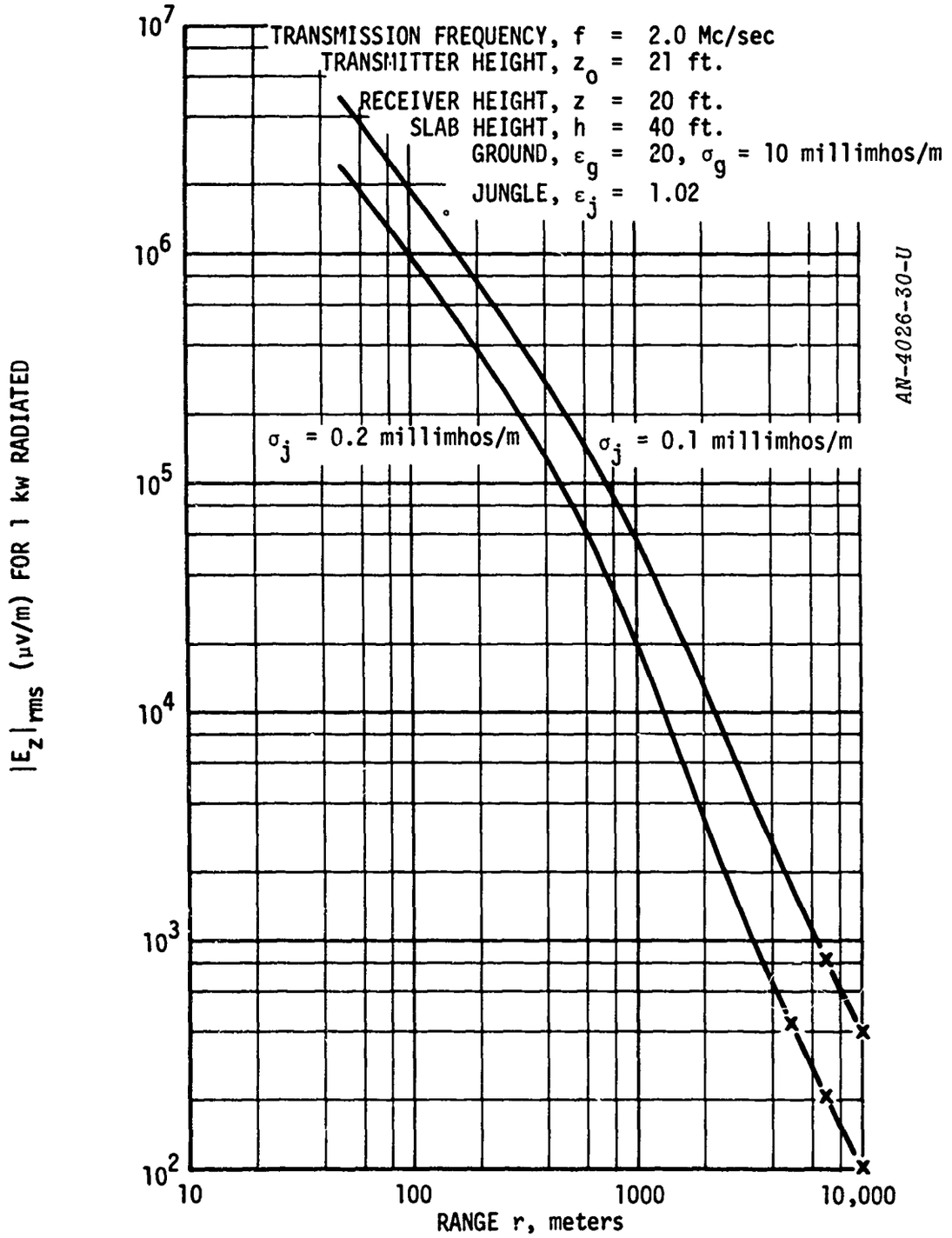

Figure 4. Sample Calculated Field for f = 2.0 Mc/sec

lateral wave described in Appendix III. For this frequency, the lateral wave is the dominant contribution throughout the range of interest. However, it is best evaluated by the method of Appendix II for $r < 5 \times 10^3$m. From Fig. 4, the lateral wave falls off slower than $1/r^2$, then faster than $1/r^2$, and finally settles to a $1/r^2$ range dependence.

The remainder of this section is concerned with a preliminary comparison of the calculated electric field with the experimental results of Jansky and Bailey.[3,4] The only case under consideration at this time is that of vertical polarization with both transmitter and receiver within the jungle. The frequency range of this comparison is from 6 to 100 Mc.

The distance from the transmitter is limited to one mile. For ranges larger than this the transmitting and receiving antenna were often separated by intervening hills, and the results do not directly apply.

The simple expression [Eq. (40), Appendix III] for the lateral wave is accurate to 3 db in the regime covered by the following graphs. The points on the graphs, however, are calculated by the Gaussian integration and are accurate to 0.1%.

For comparison purposes the calculated electric field is transformed into basic path loss,[4] L_b, by the equation

$$L_b = 139.0 - 20 \log E_{rms} + 20 \log f$$

where f is the frequency in megacycles and E_{rms} (microvolt/meter) is calculated for a point dipole radiating one kilowatt into empty space.

Figure 5 shows a series of curves of L_b vs r (miles) for various receiver heights at a given frequency, f, and transmitter height, z_o. The straight lines are calculated values for the input parameters,

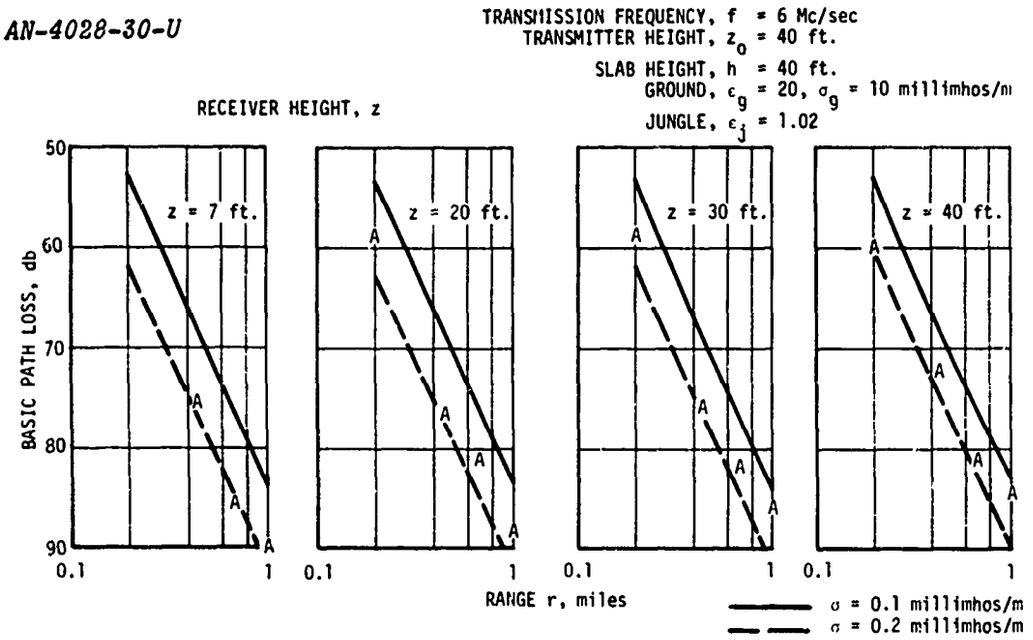

Figure 5. Comparison of Predicted and Measured Path Loss, f = 6 Mc/sec, z_o = 21 ft

h = 40 ft

ϵ_g = 15, σ_g = 10 millimho/m

and ϵ_j = 1.02

σ_j = 0.1 millimho/m for the solid line and

σ_j = 0.2 millimho/m for the dashed line.

Figures 6 through 12 are additional graphs for other combinations of f and z_o. In all graphs the experimental points are denoted by the letters A and B. These points denote measurements along two different winding trails (A and B) at the Thailand jungle test site. The scatter of the experimental data points is believed due to the lack of homogeneity of the jungle and the variation in environment of the antenna. The environment of the transmitting antenna can cause an azimuthal asymmetry in the radiation patterns. Also, the jungle character of the ray path at each azimuth may be different. Thus, there will be an azimuthal asymmetry in the electric field. Since the trails are not

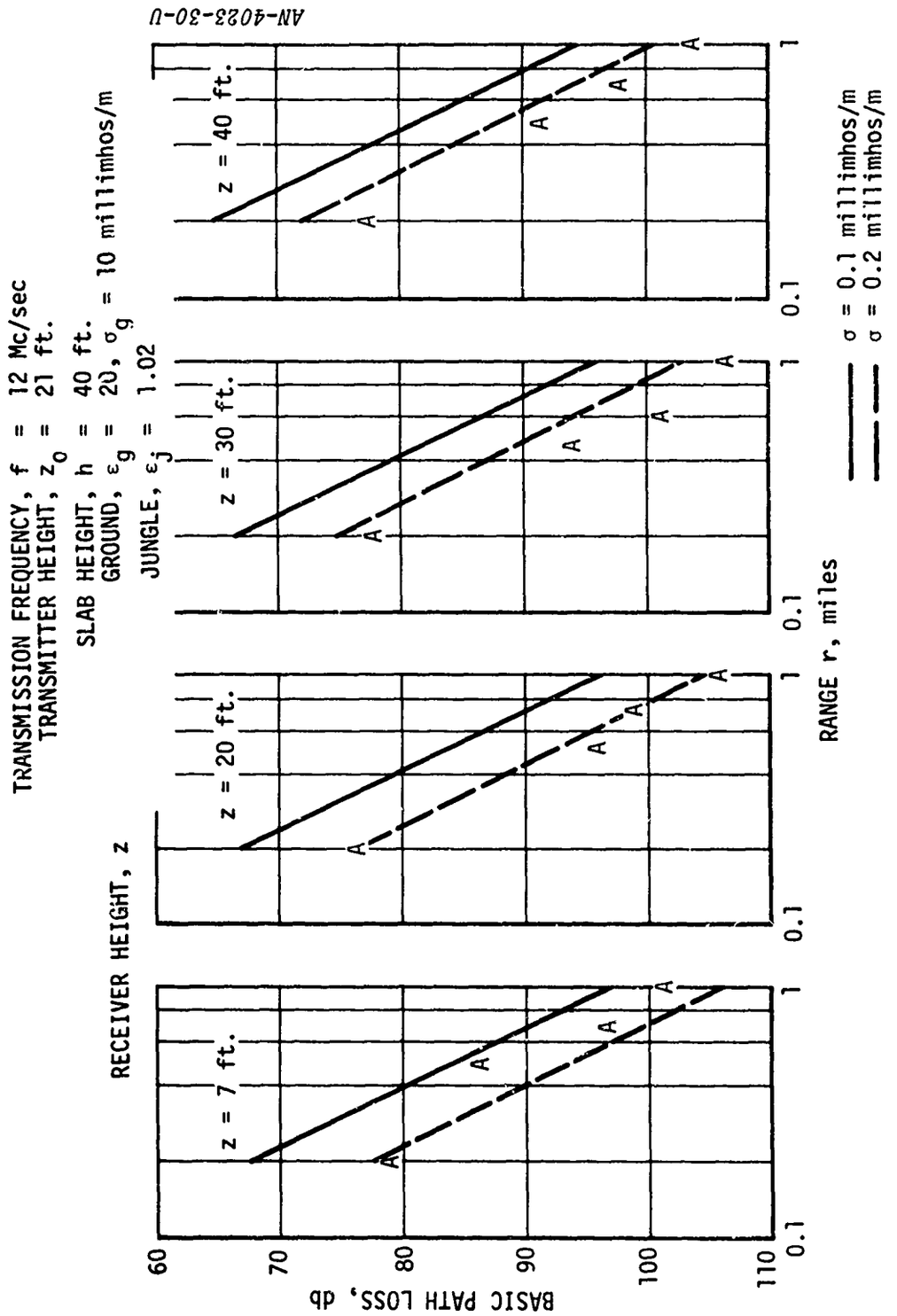

Figure 6. Comparison of Predicted and Measured Path Loss, f = 12 Mc/sec, z_o = 21 ft

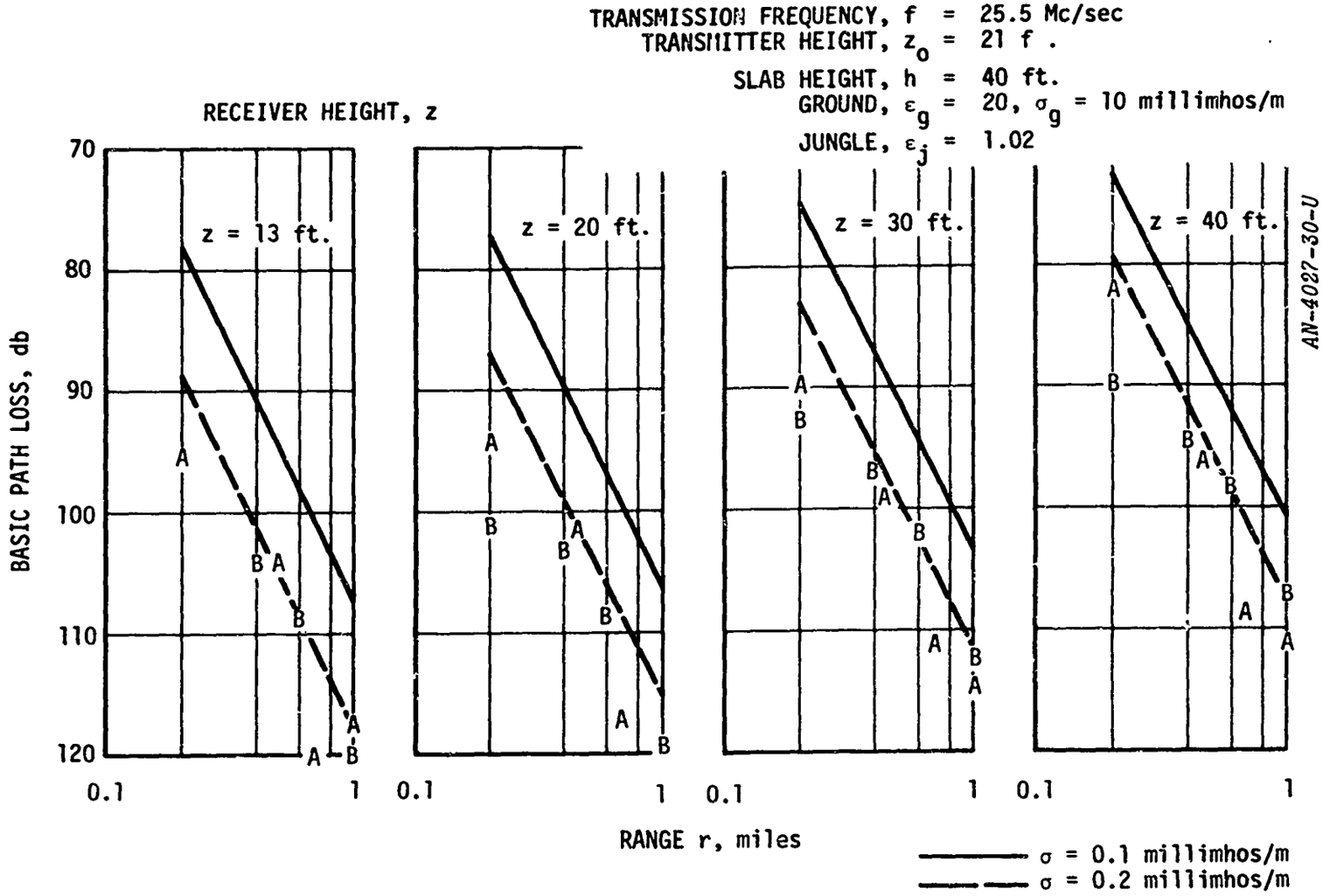

Figure 7. Comparison of Predicted and Measured Path Loss, f = 25.5 Mc/sec, z_o = 21 ft

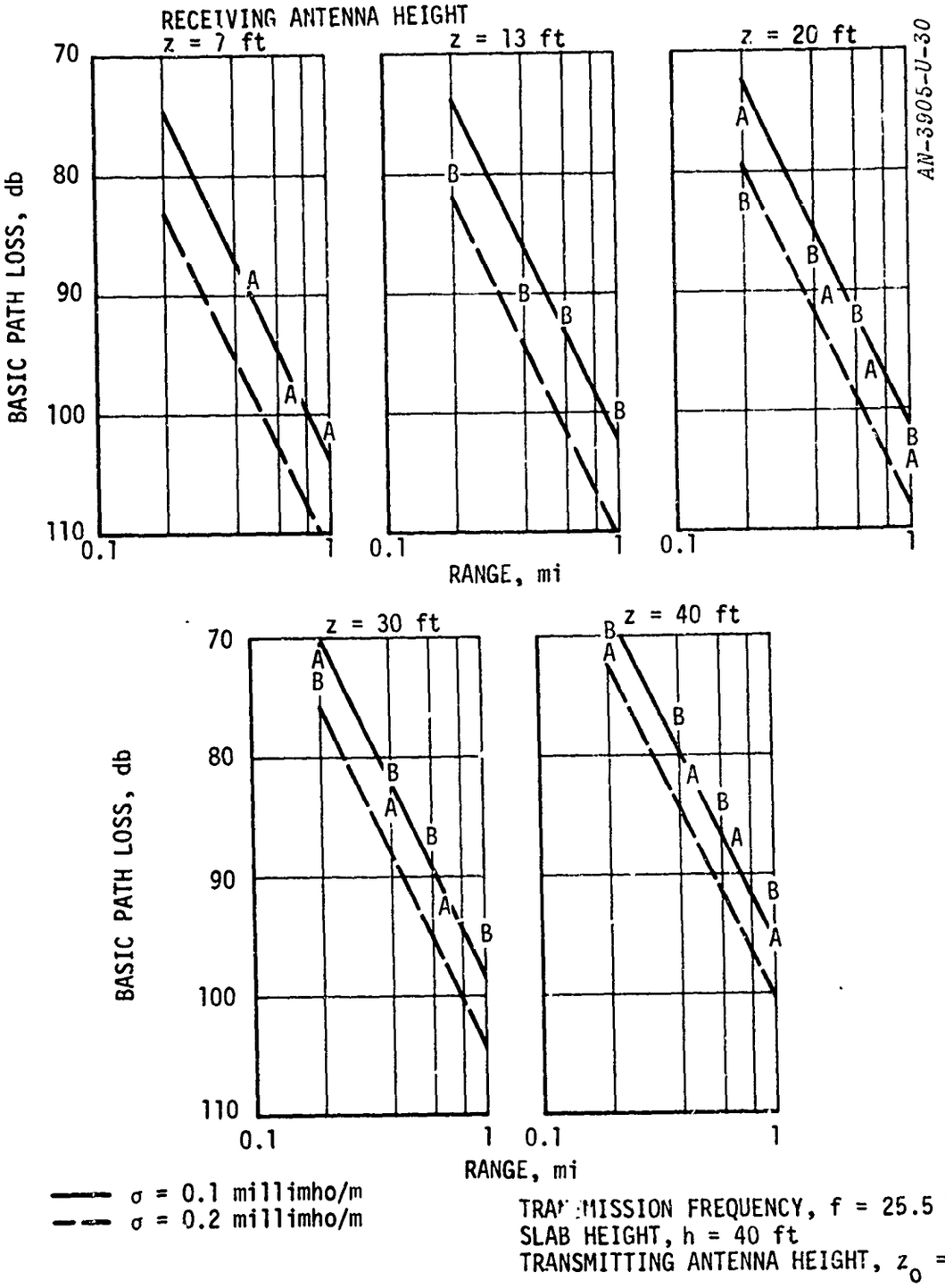

Figure 8. Comparison of Predicted and Measured Path Loss, f = 25.5 Mc/sec, z_o = 40 ft

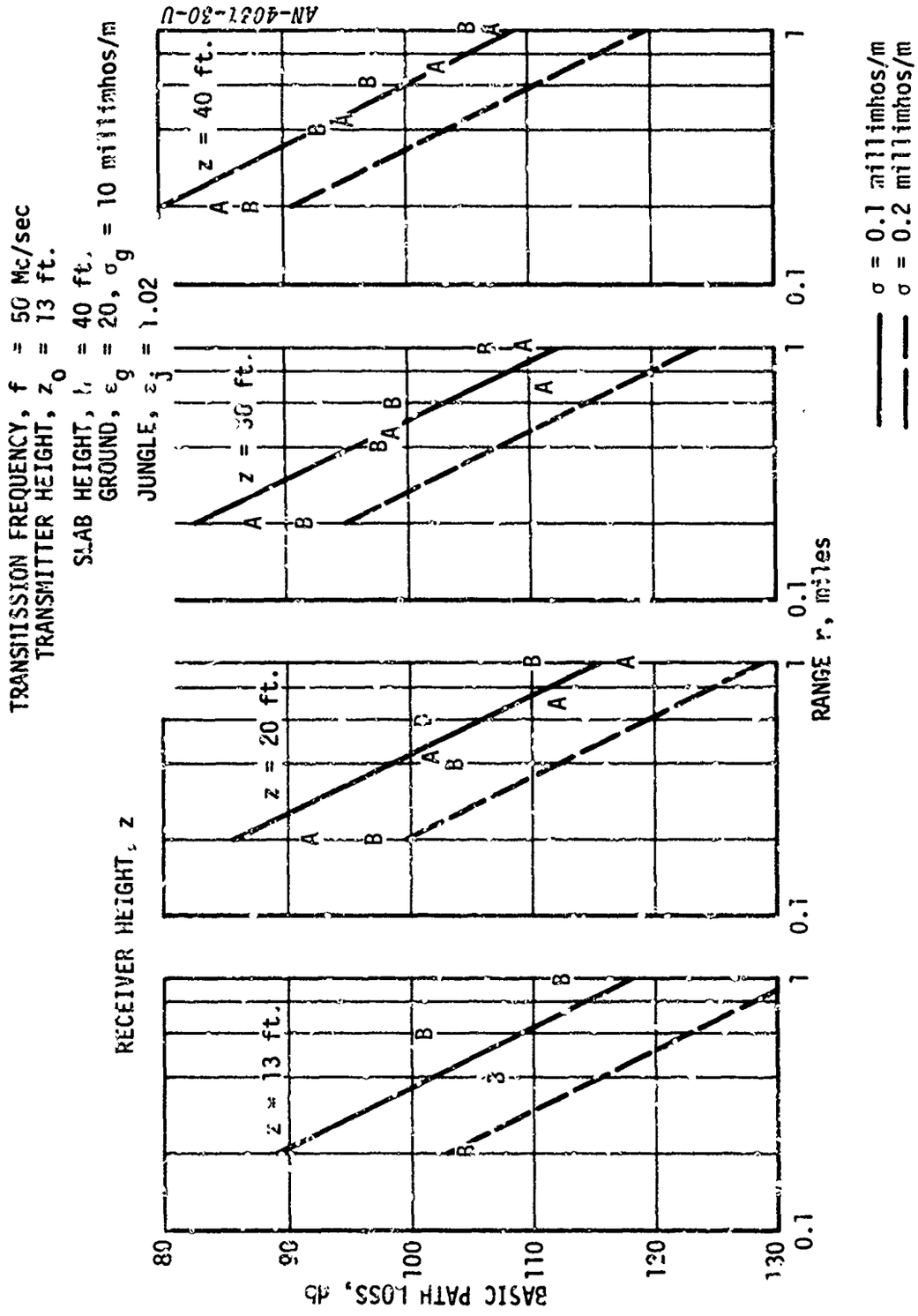

Figure 9. Comparison of Predicted and Measured Path Loss, f = 50 Mc/sec, z_o = 13 ft

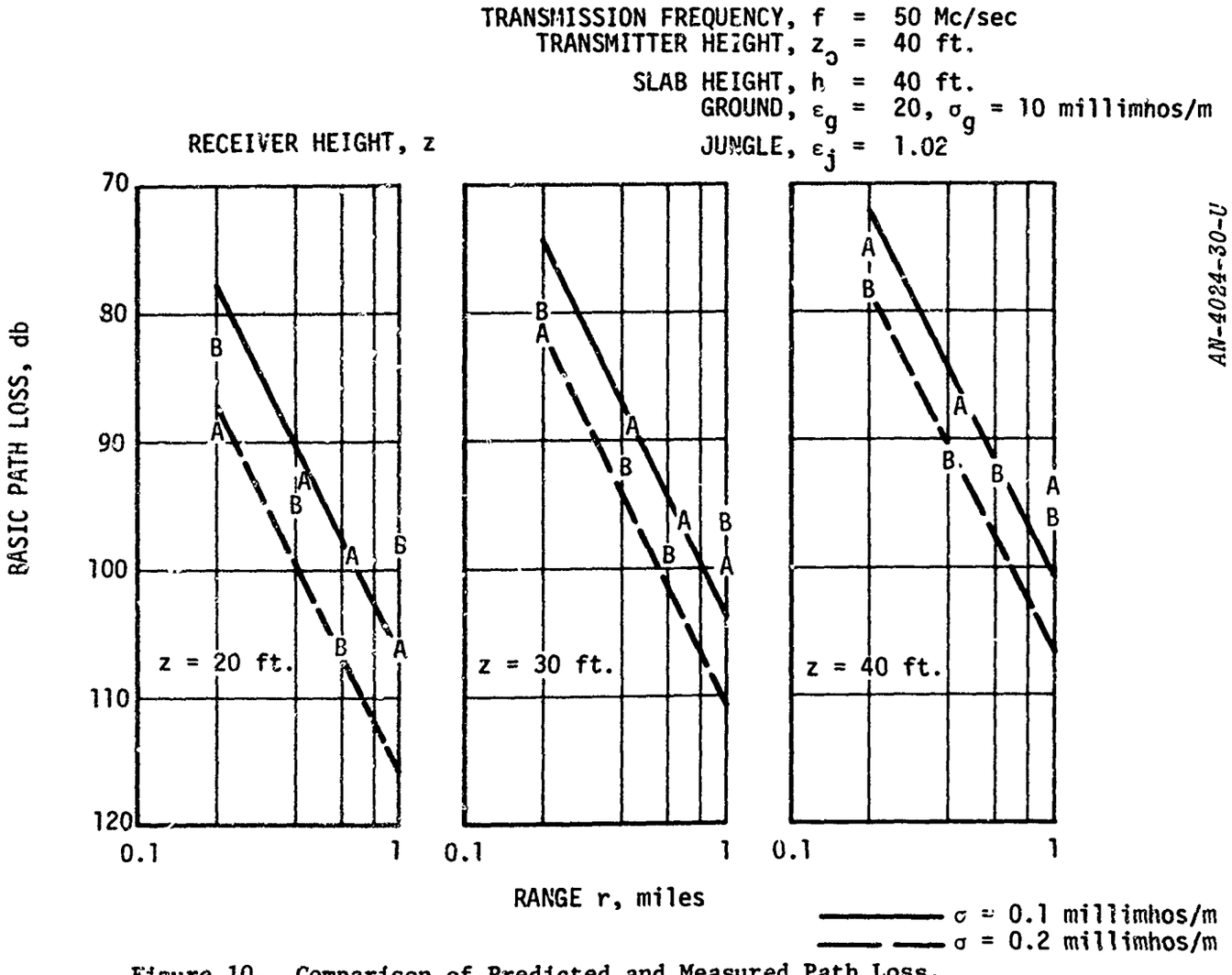

Figure 10. Comparison of Predicted and Measured Path Loss, f = 50 Mc/sec, z_o = 40 ft

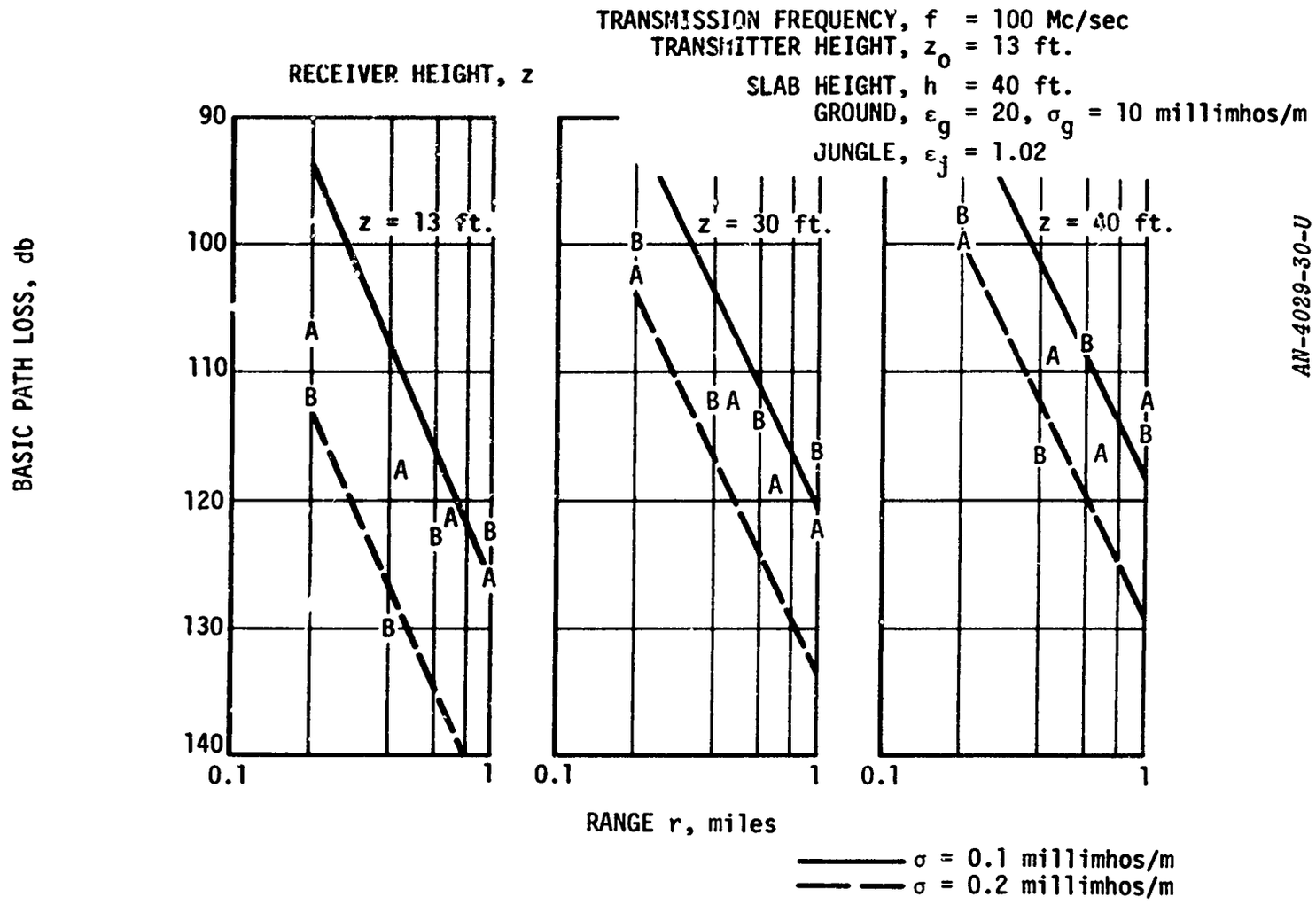

Figure 11. Comparison of Predicted and Measured Path Loss, f = 100 Mc/sec, z_o = 13 ft

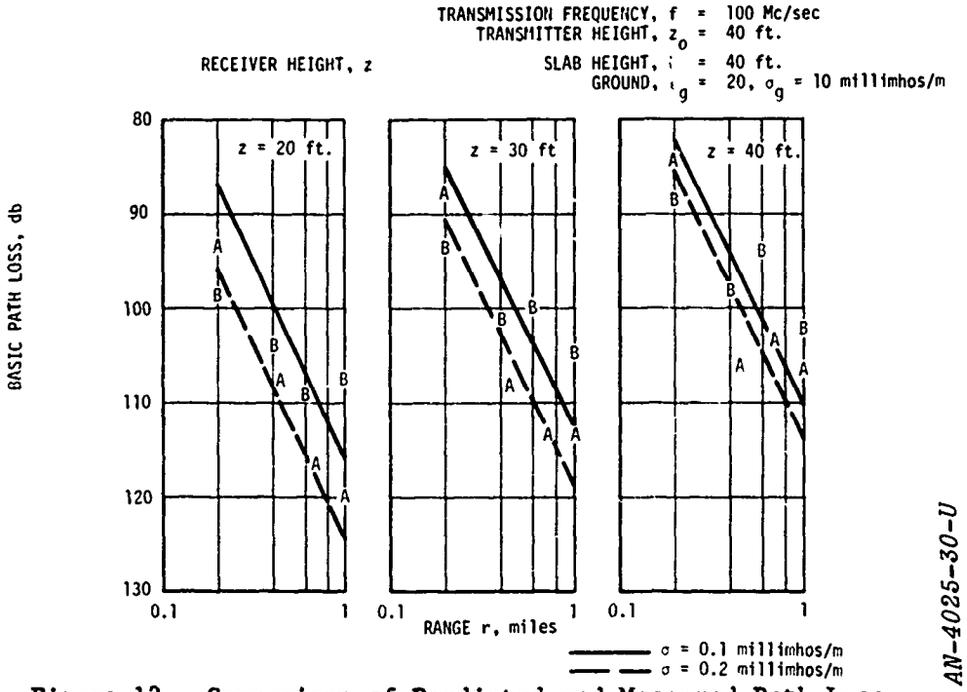

Figure 12. Comparison of Predicted and Measured Path Loss, f = 100 Mc/sec, z_o = 40 ft

straight, each measurement taken at a different range is also at a different azimuth. Finally, the receiving antenna is in a different environment at each measurement.

Since the calculated electric field depends most critically on the jungle conductivity, this was the only quantity varied in the calculations. The curves for the two values of conductivity generally bound the experimental points for all values of receiver and transmitter height and frequency with the exception of the f = 25.5 Mc, z_o = 21 ft case (Fig. 7). Jansky and Bailey,[4] on pp. 4.6 - 4.8 of Report 6, call attention to an apparent inconsistency in their data at 25.5 Mc and low transmitter height and observe that a 10 db decrease in their path loss would make their results more reasonable. This 10 db decrease in measured path loss will bring the experimental points into the neighborhood of the calculated values.

The difference between the calculated and measured path loss is plotted statistically in Fig. 13 for the two conductivities. The points of Fig. 7 were not included. These plots show the lower conductivity to predict a path loss which is too low by 4 db and the higher conductivity to predict a loss high by 5 db. The important result is the standard deviation of 6 db. This illustrates the utility of the slab model. The calculation has a 68% chance of being within 6 db of the measurement for all antenna heights, ranges and frequencies between 6 and 100 Mc when the jungle conductivity is taken as approximately 0.15 millimho/m.

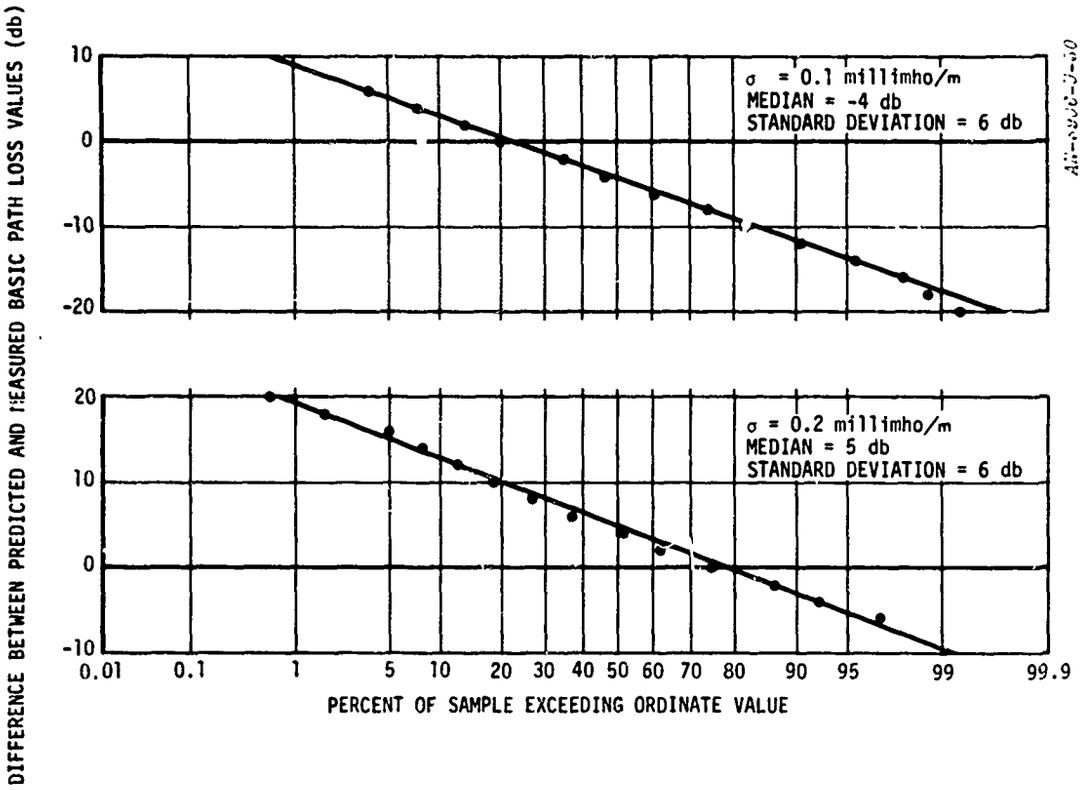

Figure 13. Distributions of Differences Between Predicted and Measured Path Loss

IV. CONCLUSIONS

A simple slab model of the jungle is capable of explaining the experimental propagation data over a wide range of parameters. The calculations performed so far have considered only vertical polarization and both antennas in the jungle. We are continuing the study to include horizontal polarization and cases where either or both of the antennas are above the jungle. A comparison with the experimental results of Jansky and Bailey and other experimental groups, where available, will be made and the regimes of validity of the slab model will be determined.

APPENDIX I

DERIVATION OF THE FIELD EXPRESSIONS

The integral representation of the fields can be obtained simply. For the sake of completeness we include an outline of the derivation following that given by Wait.[7]

The free-field equations are

$$\nabla \times E = i \frac{\omega}{c} H \tag{8}$$

$$\nabla \times H = \left(- \frac{i\omega\varepsilon}{c} + \frac{4\pi\sigma}{c}\right) E = - \frac{i\omega}{c} n^2 E$$

where $\omega = 2\pi f = cK_o$ is the angular frequency of the radiation. The fields can be expressed in terms of the Hertz vector Π

$$E = \nabla \times (\nabla \times \Pi) \tag{9}$$

$$H = - iK_o n^2 \nabla \times \Pi \tag{10}$$

if Π satisfies the equation

$$\nabla^2 \Pi + n^2 K_o^2 \Pi = 0. \tag{11}$$

Because of the cylindrical symmetry of the problem (with vertical polarization), Π is in the z-direction.

The solutions of Eq. (11) which are regular at the origin and independent of azimuth angle are

$$\Pi = J_o(\alpha R)\, e^{\pm zx} \tag{12}$$

where R is measured in units of c/ω and $x^2 = \alpha^2 - n^2$, and the real part of x is greater than zero.

The solution to our problem satisfies the free-field equations everywhere except at the antenna where it has a singularity characteristic of a point dipole. By superposition the solution has the form

$$\Pi_a = \int_o^\infty a_a(\alpha)\, J_o(\alpha R)\, e^{x_a(H-Z)}\, \alpha d\alpha \tag{13}$$

$$\Pi_j = \int_o^\infty \left[a_o e^{-x_j X} + a_j(\alpha)\, e^{x_j(H-Z)} + b_j(\alpha)\, e^{-x_j(H-Z)} \right] \frac{\alpha J_o(\alpha R)}{x_j}\, d\alpha \tag{14}$$

$$\Pi_g = \int_o^\infty b_g(\alpha)\, e^{-x_g(H-Z)}\, J_o(\alpha R)\alpha\, d\alpha \tag{15}$$

where the coefficient a_o is a measure of the dipole moments of the transmitting antenna and the other symbols have the same significance as in Section II.

By using Eqs. (9) and (10) the field components can be determined as linear functions of the four unknown functions $a_a(\alpha)$, $a_j(\alpha)$, $b_j(\alpha)$, $b_g(\alpha)$. The requirement that the tangential components of the electrical and magnetic field be continuous at the boundary leads to four algebraic equations which determine these coefficients. The algebra is straightforward and leads to

$$E_z = 2P \int_o^\infty \alpha^3\, J_o(\alpha R) F(\alpha R) d\alpha \tag{16}$$

where P and $F(\alpha R)$ are as given in Eq. (1) in the text. It is convenient to have the range of α extend from $-\infty$ to $+\infty$. To do this we note that $F(-\alpha) = -F(\alpha)$ and

$$J_o(\alpha R) = \frac{1}{2}\left[H_o^{(1)}(\alpha R) - H_o^{(1)}(-\alpha R)\right].$$

With these substitutions we obtain Eq. (1) of the text.

APPENDIX II

EXPLICIT EVALUATION OF THE FIELD INTEGRAL

The explicit evaluation of the field integral given by Eq. (1) of Section II cannot be achieved by conventional quadrature techniques because of the rapid oscillation of the Bessel function for large αR. Thus even though the function $F(\alpha)$ converges in general within modest ranges of α, most numerical integration procedures would lose all significance whenever R became appreciable because of the cancellation of the individual quadrature terms with one another. For any well-behaved $F(\alpha)$ the integral is easily shown to tend to zero as R tends to infinity. Via numerical quadrature, this would be manifest by a large number of terms of essentially equal magnitude (though different sign) being added together to yield a residual which may be made as small as desired by letting R become large. Irrespective of the number of significant figures a given digital computer is capable of handling, there will always exist an R beyond which a mechanical quadrature will result in a total loss of significance. There is, however, a means of numerically evaluating the integral in question without meaningful loss of accuracy for any value of R so long as computing time is no obstacle. In other words, a numerical attack upon the integral is always possible, but becomes more time-consuming as R increases. The broad range of validity for the analytic methods of Section III, however, insures that these contingencies do not arise. Of particular note concerning the numerical evaluation described herein is its exact agreement with the results of Section III in the regime beyond which the latter approach was shown to be accurate. Thus two essentially independent evaluations of the integrals concerned yield identical results, thereby providing a self-consistency check rarely available in similar work. In regimes where the methods of Section III are no longer accurate, those described in this appendix are used; and conversely, where these numerical quadratures become too time-consuming, the analytic methods of Section III are of sufficient accuracy to be used.

A mechanical quadrature of the field integral is achieved by first noting that the source term contribution may be evaluated explicitly . Thus

$$E_z = E_z^{prim} + A \int_0^\infty [f_1(\alpha) + f_2(\alpha)]\, J_o(\alpha R)\alpha^3 d\alpha \qquad (17)$$

where

$$E_z^{prim} = A \frac{e^{in_j Q}}{Q}\left[n_j^2 + \frac{1}{Q}\left\{ \frac{R^2 - 2(Z-Z_o)^2}{Q^2}\, in_j - 1/Q \right.\right.$$

$$\left.\left. - \frac{n_j^2 (Z-Z_o)^2}{Q} \right\} \right] , \qquad (18)$$

and

$$Q = \sqrt{R^2 + (Z-Z_o)^2} \quad , \qquad (19)$$

with $f_1(\alpha)$ and $f_2(\alpha)$ given in appendix I.

When α^2 becomes somewhat larger than the modulus of n_j^2, the dominant behavior of $f_1(\alpha)$ is controlled by the exponential factor

$$e^{-x_j Y} \rightarrow e^{-\alpha Y} \qquad (20)$$

whereas $f_2(\alpha)$ is dominated by the factor

$$e^{-x_j (2H-Y)} \rightarrow e^{-\alpha(2H-Y)} \quad . \qquad (21)$$

Thus given h, z, z_o, and f (See Sec. II for nomenclature) an upper limit of α (called α_{max}) may be chosen beyond which the integrand of Eq. (17) contributes a negligible amount. This α_{max} will be sufficient for a

complete range of R. If R is fixed, on the other hand (i.e., the generation of height gain curves is required), α_{max} must be varied in such a way that α_{max} Y is greater than a fixed constant. Since Y and H are directly proportional to the propagation frequency, α_{max} is easily frequency scaled.

All that remains, therefore, is the evaluation of

$$E_z^{sec} = A \int_0^{\alpha_{max}} [f_1(\alpha) + f_2(\alpha)]\, J_o(\alpha R)\alpha^3 d\alpha \qquad (22)$$

where $f_1(\alpha)$ and $f_2(\alpha)$ are complex functions. Separating each into real and imaginary parts, the secondary field may still be written in terms of finite integrals along the real α-axis as

$$E_z^{sec} = A \left[\int_0^{\alpha_{max}} g_1(\alpha)\, J_o(\alpha R)\alpha^3 d\alpha + i \int_0^{\alpha_{max}} g_2(\alpha)\, J_o(\alpha R)\alpha^3 d\alpha \right] \qquad (23)$$

where $g_1(\alpha) = \mathrm{Re}[f_1(\alpha) + f_2(\alpha)]$ and $g_2(\alpha) = \mathrm{Im}\,[f_1(\alpha) + f_2(\alpha)]$.

The severe oscillations of $J_o(\alpha R)$ do not occur until αR is well beyond unity. Indeed at this point $J_o(\alpha R)$ can be accurately replaced by the first two terms of its asymptotic expansion, viz.

$$J_o(\alpha R) \sim \sqrt{\frac{2}{\pi \alpha R}} \left[\cos(\alpha R - \pi/4) + \frac{\sin(\alpha R - \pi/4)}{8\alpha R} \right]. \qquad (24)$$

This expansion will provide an approximation to $J_o(\alpha R)$ better than one part in 10^4 when $\alpha R > 30$. Choosing $\beta = 30/R$ the integrals of Eq. (23) may be divided into two parts, viz.

$$\int_0^{\alpha_{max}} d\alpha = \int_0^{\beta} d\alpha + \int_{\beta}^{\alpha_{max}} d\alpha \,, \qquad (25)$$

with the asymptotic representation of $J_o(\alpha R)$ being used in the last integral. The integrals from 0 to β may be very accurately generated using standard Gaussian quadratures whereas the integrals from β to α_{max} are most amenable to solution by Filon's method.[9] This latter method, described in considerable detail in references 9 and 10, was developed to handle mechanical quadratures of the type

$$\int_a^b f(x) \cos Rx \, dx \tag{26}$$

Upon substituting (24) into (23) for $\alpha > \beta$, the resulting integrals may be cast into one of the forms

$$\int_\beta^{\alpha_{max}} F_1(x) \cos (Rx - \pi/4)dx \text{ or } \int_\beta^{\alpha_{max}} F_2(x) \sin(Rx - \pi/4)dx \tag{27}$$

The interval from β to α_{max} is then divided into 2n equal intervals of size $\delta = (\alpha_{max} - \beta)/2n$ and the values of the independent variable α at these points are indicated by $x_o, x_1, \ldots, x_{2n}$. Introducing the variable $\theta = \delta R$, one obtains

$$\int_{x_o}^{x_{2n}} F(\alpha) \cos(\alpha R - \pi/4)d\alpha$$

$$= \delta \left[p(\theta) \left\{ F_{2n} \sin\left(Rx_{2n} - \frac{\pi}{4}\right) - F_o \sin\left(Rx_o - \frac{\pi}{4}\right) \right\} \right.$$

$$\left. + q(\theta)C_{2n} + r(\theta)C_{2n-1} \right] + R_n \tag{28}$$

and

$$\int_{x_o}^{x_{2n}} F(\alpha)\,\sin(\alpha R - \pi/4)\,d\alpha$$

$$= \delta\Big[p(\theta)\,\Big\{F_o\cos\Big(Rx_o - \frac{\pi}{4}\Big) - F_{2n}\cos\Big(Rx_{2n} - \frac{\pi}{4}\Big)\Big\}$$

$$+ q(\theta)\,S_{2n} + r(\theta)S_{2n-1}\Big] + R_n' \qquad (29)$$

where the generalized Simpson coefficients p, q, and r are given by

$$p(\theta) = \frac{1}{\theta} + \frac{\sin 2\theta}{2\theta^2} - \frac{2\sin^2\theta}{\theta^3} \qquad (30)$$

$$q(\theta) = 2\left(\frac{1+\cos^2\theta}{\theta^2} - \frac{\sin 2\theta}{\theta^2}\right) \qquad (31)$$

$$r(\theta) = 4\left(\frac{\sin\theta}{\theta^3} - \frac{\cos\theta}{\theta^2}\right) \quad . \qquad (32)$$

In addition, one has

$$C_{2n} = \sum_{i=0}^{n} F_{2i}\cos\,(Rx_{2i} - \pi/4)$$

$$- \frac{1}{2}\left[F_{2n}\cos\,(Rx_{2n} - \pi/4) + F_o\cos\,(Rx_o - \pi/4)\right] \qquad (33)$$

$$C_{2n-1} = \sum_{i=1}^{n} F_{2i-1}\cos\,(Rx_{2i-1} - \pi/4) \qquad (34)$$

$$S_{2n} = \sum_{i=0}^{n} F_{2i}\sin\,(Rx_{2i} - \pi/4) - \frac{1}{2}\,[F_{2n}\sin\,(Rx_{2n} - \pi/4)$$

$$+ F_o\sin\,(Rx_o - \pi/4)] \qquad (35)$$

$$S_{2n-1} = \sum_{i=1}^{n} F_{2i-1} \sin (Rx_{2i-1} - \pi/4). \tag{36}$$

The remainder terms are given by

$$R_n = \frac{2}{45} Rh^5 \sum_{i=1}^{n} F^{(3)}_{2i-1} \sin (Rx_{2i-1} - \pi/4) - \frac{nh^5}{90} F^{(4)}(\xi) - O(Rh^7) \tag{37}$$

$$R'_n = \frac{2}{45} Rh^5 \sum_{i=1}^{n} F^{(3)}_{2i-1} \cos (Rx_{2i-1} - \pi/4) - \frac{nh^5}{90} F^{(4)}(\xi) - O(Rh^7) \tag{38}$$

As is evident from expressions (37) and (38), the error is proportional to R times the interval size to the fifth power. Thus for very large R the interval size h must be decreased appropriately to maintain accuracy. This in turn results in increasingly long periods of computation. The true practical usefulness of Filon's method is therefore in some doubt. Although postulated to be a panacea for large R, the method is actually most useful from the practical point of view for small θ, i.e., for hR small. With a computer, however, the method does yield a convergent solution as the interval size h tends to zero. This should be contrasted to any other mechanical quadrature scheme which, irrespective of the smallness of the integration step size, will in general not converge for any reasonably large value of R.

APPENDIX III

ANALYTIC SOLUTIONS

In order to obtain an asymptotic expansion of the fields we first note that $H_o^{(1)}$ has the asymptotic expansion

$$H_o^{(1)}(\alpha R) = \sqrt{\frac{2}{\pi\alpha R}}\, e^{-i\pi/4}\, e^{i\alpha R}\left(1 + \frac{1}{8i\alpha R} + 0\left(\frac{1}{R^2}\right)\right)$$

valid for $|\alpha R| >> 1$. This may then be inserted into Eq. (1) of the text and the resulting integral can be evaluated as a contour integral.

The integrand vanishes on an infinite semi-circle in the upper half α-plane because of the $e^{i\alpha R}$ term in $H_o^{(1)}$. The original contour which lay along the real axis is therefore deformed to this semi-circle. One is left with integrals along two branch cuts and contributions from poles that were crossed (Fig. 14).

The poles correspond to transmission modes through the jungle which are exponentially damped. The cut at $x_g = 0$ ($\alpha = n_g$) corresponds to the lateral wave at the jungle-ground boundary. This wave is highly attenuated because of the high conductivity of the ground and is negligible. The cut at $x_a = 0$ ($\alpha = 1$) corresponds to the lateral wave at the jungle-air boundary. This wave is not exponentially attenuated and is therefore the dominant contribution after one damping length of the pole terms. There is no branch point at $x_j = 0$ ($\alpha = n_j$) since F is even in x_j.

The poles are the normal modes of propagation through a waveguide and would be the dominant contribution if the waveguide were not a lossy jungle. In this case these pole contributions are negligible for

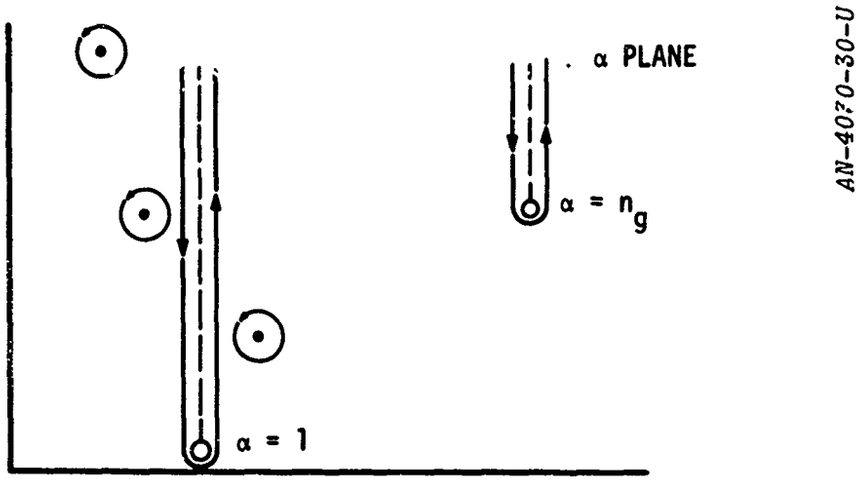

Figure 14. Contours in the Complex α-Plane

distances greater than a jungle wavelength. The cut at $\alpha = 1$ corresponds to that part of the source radiation which is transmitted from the jungle to the air above and then propagates through the air. This is analogous to the usual ground or surface wave of radio propagation except in this case the lower boundary is jungle rather than ground.

The contribution from the cut at $\alpha = 1$ is evaluated by transforming to the variable s by the transformation $\alpha = 1 + is^2$; $-\infty \leq s \leq \infty$. This transformation describes the contour of the α-plane which runs from $\alpha = 1 + i\infty$ to $\alpha = 1$ on the left of the cut as the negative real s axis and the contour in the α-plane which runs from $\alpha = 1$ to $\alpha = 1 + i\infty$ on the right side of the cut as the positive real s axis.

By taking

$$x_a = \sqrt{\alpha^2 - 1} = s(i + 1) \sqrt{1 + is^2/2}$$

the correct sign for x_a on each side of the cut obtains.

With this transformation the branch cut contribution is

$$E_z^b = P\sqrt{\frac{8}{\pi R}}\, e^{i\pi/4}\, e^{iR} \int_{-\infty}^{\infty} ds(1 + is^2)^{5/2}\, s\, e^{-Rs^2} F(\alpha(s))\left(1 + \frac{1}{8iR(1+is^2)} + \ldots\right) \tag{39}$$

The functions F(s) and $(1 + is^2)^m$ where m = -1 and 5/2 are expanded in Taylor series about s = 0. Only terms of the integrand that are even in s survive. The result is

$$E_z^b = \frac{\sqrt{2i}\; e^{iR}\, P}{R^2}\left[F_o' + \frac{29iF_o'}{8R} + \frac{F_o'''}{4R} + 0\left(\frac{1}{R^2}\right)\right]$$

where the subscript "o" means the derivatives are evaluated at s = 0. The expression for E_z^b is an asymptotic expansion in R. The $\frac{1}{R}$ terms in the bracket provide an estimate of the error involved when using the first term alone. The result is then

$$E_{rms} = \frac{|PF_o'|}{R^2}$$

$$= \frac{9\cdot 10^{10}\sqrt{\text{Power}}}{\sqrt{2\pi f}\,|n^2-1|r^2} \quad K(Z, Z_o, H)\ \mu\text{volt/m} \tag{40}$$

where

$$K(Z,Z_o,H) = \left|\frac{\left[e^{x_j^o Z_o} + V_g^o e^{-x_j^o Z_o}\right]\left[e^{x_j^o Z} + V_g^o e^{-x_j^o Z}\right]}{\left[e^{x_j^o H} - V_g^o e^{-x_j^o H}\right]^2}\right|$$

and

$$V_g^o = \frac{n_g^2 x_j^o - n_j^2 x_g^o}{n_g^2 x_j^o + n_j^2 x_g^o} \quad , \quad x_g^o = \sqrt{1 - n_g^2} \text{ and } x_j^o = \sqrt{1 - n_j^2} \quad .$$

The fractional error is

$$E = \left| \frac{29i}{8R} + \frac{F_o'''}{4RF_o'} \right| = \left| E_1 + E_2 + E_3 + E_4 + E_5 \right| \tag{41}$$

where

$$E_1 = \frac{-3h}{rx_j^o} \left[\frac{1 + V_g^o e^{-2x_j^o H}}{1 - V_g^o e^{-2x_j^o H}} \right]$$

$$E_2 = \frac{\left(3n_j^2 - 1\right)}{R}$$

$$E_3 = \frac{12n_j^4 V_g^o e^{-2x_j^o H}}{R\left(n_j^2 - 1\right)\left(1 - V_g^o e^{-2x_j^o H}\right)^2}$$

$$E_4 = \frac{3}{2Rx_j^o} \left[\frac{Y\left(e^{x_j^o Y} - V_g^{o\,2} e^{-x_j^o Y}\right) + XV_g^o \left(e^{-x_j^o X} + e^{x_j^o X}\right)}{e^{x_j^o Y} + V_g^{o\,2} e^{-x_j^o Y} + V_g^o \left(e^{-x_j^o X} + e^{x_j^o X}\right)} \right]$$

$$E_5 = \frac{3n_j^2 n_g^2 (n_g^2 - n_j^2)}{R\, x_j^o x_g^o (n_g^2 x_j^o + n_j^2 x_g^o)^2} \times$$

$$\left[\frac{e^{-x_j^o X} + e^{x_j^o X} + 2V_g^o e^{-x_j^o Y}}{e^{x_j^o Y} + V_g^{o\,2} e^{-x_j^o Y} + V_g^o \left(e^{-x_j^o X} + e^{x_j^o X}\right)} + \frac{2e^{-2x_j^o H}}{1 - V_g^o e^{-2x_j^o H}} \right]$$

This expression is too complicated to be useful if a quick estimate of the error involved in using Eq. (40) is desired. Comparison with a numerical evaluation of the branch-cut integral, Eq. (39), shows that the discrepancy between Eq. (40) and the exact evaluation agrees with the estimated error only at the high frequencies ($f \geq 25.5$ Mc). At $f < 25.5$ Mc, the discrepancy is greater than the estimated error by a factor of three in some cases. It would therefore be desirable to replace the error expression, Eq. (41), by a simpler and more accurate error bound. Numerical work shows that the expression for the error may be approximated by the following formula:

$$E = \left| \frac{3\, n_j^4}{R(n_j^2 - 1)} \right| + \left| \frac{3\,(H - Y/2)}{R\, x_j^o} \right| \qquad (42)$$

for frequencies in the range $6 < f < 100$ Mc. However, this expression is overly pessimistic at the high frequencies and is too small for $f < 6$ Mc. An accurate error bound at all frequencies can be obtained by simply using three times E (expression 41). More extensive numerical comparisons will be necessary in order to determine simpler expressions for accurate error bounds in all frequency regions.

Both expressions (41) and (42) show the error to be inversely proportional to r. The error decreases as the range increases. Thus the long-range behavior of the electric field is accurately given by expression (40).

When $E \approx 1$, expression (40) is no longer accurate but the integrand of Eq. (39) is still well-behaved so that a Gaussian integration of Eq. (39) is easily effected. In this regime, the branch cut is still the dominant contribution. However, it is evaluated numerically to an accuracy of 0.1% rather than by the asymptotic expansion.

For E > 1, the Gaussian integration fails to converge. In this regime a numerical integration of the original integral is used. The numerical integration is accomplished by a machine code, described in Appendix II, which evaluates the total field, that is, the contribution from the cuts and all poles. We thus are in a position to make an accurate numerical evaluation of E_z for all values of the input parameters.

REFERENCES

1. J.W. Herbstreit and W.Q. Crichlow, Measurement of Factors Affecting Jungle Radio Communication, Office of Chief Signal Officer, Operation Research Branch, ORB-2-3, November 1943 (UNCLASSIFIED).

2. B.A. Lippmann, The Jungle as a Communication Network, Defense Research Corp. IMR-168/1, August 1965 (UNCLASSIFIED).

3. Tropical Propagation Research, Jansky and Bailey, Semi-Annual Report No. 4, DA36-039 SC 90889, 1964 (UNCLASSIFIED).

4. Ibid, Semi-Annual Reports No's. 5 and 6, 1964-1965.

5. L.M. Brekhovskikh, Waves in Layered Media, translated by David Lieberman, edited by Robert T. Beyer (Academic Press, New York, 1960).

6. J. R. Wait, Electromagnetic Waves in Stratified Media, (Pergamon Press, London 1963).

7. J. R. Wait, J. of Res. N.B.S. 59, 365 (1957).

8. G.H. Hagn, B.H.W. Parker, Proceedings of the 1966 Spring Meeting of the International Scientific Radio Union, National Academy of Sciences, p. 40.

9. L.N.G. Filon, Proc. Roy. Soc. Edinburgh (A) 49, 38 (1928).

10. Handbook of Mathematical Functions, NBS Appl. Math. Ser 55 (1964), pp. 890-891.

UNCLASSIFIED
Security Classification

DOCUMENT CONTROL DATA - R & D

(Security classification of title, body of abstract and indexing annotation must be entered when the overall report is classified)

1. ORIGINATING ACTIVITY (Corporate author)

General Research Corporation
P.O. Box 3587, Santa Barbara, California 93105

2a. REPORT SECURITY CLASSIFICATION
UNCLASSIFIED

2b. GROUP

3. REPORT TITLE

A Conducting-Slab Model for Electromagnetic Propagation Within a Jungle Medium

4. DESCRIPTIVE NOTES (Type of report and inclusive dates)
Technical Memorandum 376

5. AUTHOR(S) (First name, middle initial, last name)

D. L. Sachs and P. J. Wyatt

6. REPORT DATE	7a. TOTAL NO. OF PAGES	7b. NO. OF REFS
May 1966	44	10

8a. CONTRACT OR GRANT NO.	9a. ORIGINATOR'S REPORT NUMBER(S)
DA-31-124-ARO-D-312, ARPA Order 632	TM-376
b. PROJECT NO.	
c.	9b. OTHER REPORT NO(S) (Any other numbers that may be assigned this report)
d.	

10. DISTRIBUTION STATEMENT
Distribution of this document is unlimited.

11. SUPPLEMENTARY NOTES	12. SPONSORING MILITARY ACTIVITY
	Advanced Research Projects Agency The Pentagon Washington, D.C.

13. ABSTRACT

A theoretical determination of the path loss in radio propagation through jungle is obtained by considering the jungle as a homogeneous conducting dielectric slab on a flat earth. An exact integral is obtained for the vertical component of the electric field within the jungle due to a vertical electric dipole within the jungle. An analytic evaluation of the integral leads to an approximate expression for the field and an estimate of the error. When this accuracy is insufficient, a numerical evaluation of the integral is performed. The combination of analytic and numerical techniques leads to the evaluation of the electric field and thereby path loss to any accuracy desired. Experimental measurements of path loss in a Thailand jungle are compared with the calculations. The results agree within a standard deviation of 6 db when the jungle conductivity is taken as 0.15 millimho/m.

DD FORM 1 NOV 65 1473

UNCLASSIFIED
Security Classification